Electronic Supplementary Material (ESI) for Physical Chemistry Chemical Physics.
This journal is © the Owner Societies 2022

# Supporting Information

# Elucidating the Enhanced Decomposition of Alkyl Hydroperoxides on Oxygen Vacancy Rich $TiO_{2-x}$ Surfaces using DFT for Polyethylene Decomposition

*Yong Jieh Lee,[a] Lutfi Kurnianditia Putri,[a] Boon-Junn Ng,[a] Lling-Lling Tan,[a] Ta Yeong Wu,[a] and Siang-Piao Chai*[a]*

[a]Multidisciplinary Platform of Advanced Engineering, Chemical Engineering Discipline, School of Engineering, Monash University, Jalan Lagoon Selatan, 47500 Bandar Sunway, Selangor, Malaysia.

*Author to whom correspondence should be addressed: *chai.siang.piao@monash.edu*

## 1. Computational Methods

Density functional theory (DFT) calculations were performed using Vienna *ab initio* simulation package (VASP).[1, 2] A 3 x 3 surface slab supercell of $TiO_2$ and $TiO_{2-x}$ anatase were used for adsorption studies to ensure sufficient separation between adsorbates in adjacent supercells, thus preventing unintended adsorbate-adsorbate interactions. The lattice parameters of the surface slab were a = 10.210 Å, b = 11.328 Å, c = 29.353 Å with a slab thickness of ~8 Å. The {101} facet surface was chosen due to its prevalence on the anatase surface as shown in the Wulff construction,[3] and the subsurface oxygen vacancy position was used in the $TiO_{2-x}$ model due to its stability.[4] Due to the infeasibility of simulating a polyethylene hydroperoxide macromolecule with large number of atoms, sec-pentyl hydroperoxide was chosen as the model adsorbate, which sufficiently describes the nature of hydroperoxide functional group on the secondary position of the polymer backbone. A vacuum layer of ~20 Å perpendicular to the surface was also employed to prevent spurious interactions between the periodic slabs.

The exchange and correlation potential was described using Perdew-Burke-Ernzerhof (PBE) parameterization of generalized gradient approximation (GGA) level of theory.[5] The plane wave basis set cut-off energy was set at 520 eV, and pseudopotentials were resolved using projector augmented wave (PAW) frozen core model.[6, 7] The Brillouin zone was sampled with (3 x 3 x 1) Monkhorst-Pack scheme of kpoint mesh to carry out numerical integration in the reciprocal space.[8] Computation was performed with criterion of $10^{-5}$ eV and 0.04 eV/Å for electronic self-consistent field calculations and Hellmann-Feynman forces respectively. The adsorption energy ($E_{ads}$) was calculated according to Eq. 1.

$$E_{ads} = E_{(adsorbate-surface)} - E_{adsorbate} - E_{surface} \quad (1)$$

where $E_{(adsorbate-surface)}$ is the total energy of sec-pentyl hydroperoxide adsorbed onto the $TiO_2$ or $TiO_{2-x}$ surface, $E_{adsorbate}$ is the total energy of isolated sec-pentyl hydroperoxide, and $E_{surface}$ is the total energy of the $TiO_2$ or $TiO_{2-x}$ relaxed surface slab. Bader charge analysis[9] was performed using Henkelman's code to integrate electron densities per unit atom basins.[10] Transition state and activation energy were also investigated using climbing image nudged elastic band (CI-NEB) method.[11]

Density of states calculation were converged with more stringent parameters. $TiO_2$ and $TiO_{2-x}$ surface structures were modelled with a 1 x 3 surface slab having a slab thickness of ~8 Å and a vacuum layer of ~20 Å, with anatase {101} facet and subsurface oxygen vacancy for $TiO_{2-x}$. The lattice parameters of the surface slab were a = 10.210 Å, b = 3.776 Å, c = 29.353 Å. Exchange correlation potentials, basis sets and pseudopotentials were the same as before (*vide supra*). The Brillouin zone was sampled with (4 x 4 x 1) Monkhorst-Pack scheme of kpoint mesh to carry out numerical integration in the reciprocal space.[8] Computation was performed with criterion of $10^{-6}$ eV and 0.01 eV/Å for spin polarized electronic self-consistent field calculations and Hellmann-Feynman forces respectively. Spurious self-interaction errors from Ti 3d shells were resolved utilizing on-site Coulombic interactions employed via the Hubbard *U* correction (GGA+U) [12], following the Dudarev method of implementation [13]. Hubbard parameter of $U = 4$eV for Ti species was selected as it best describes and reproduces the *d* electron localized nature of the defect states in $TiO_{2-x}$ [14]. Calculations of d-band center was implemented according to Eq. 2.[15]

$$\varepsilon_d = \frac{\int_{-\infty}^{\infty} n_d(\varepsilon)\varepsilon \, d\varepsilon}{\int_{-\infty}^{\infty} n_d(\varepsilon) \, d\varepsilon} \tag{2}$$

where $n_d(\varepsilon)$ is the DOS of 3d orbitals of the surface Ti atoms at a given energy $\varepsilon$.

## 2. Experimental Methods

### 2.1 Chemicals and Materials

Titanium (IV) fluoride, polyethylene powder and sodium hydroxide were obtained from Sigma Aldrich. Titanium (III) chloride 30% solution and cyclohexane were obtained from Merck. Absolute ethanol was obtained from J. T. Baker. All chemicals were used as received without any further purification.

### 2.2 Photocatalyst Synthesis

$TiO_{2-x}$ was synthesized via solvothermal method. Briefly, $TiF_4$ was dissolved in 5ml of absolute ethanol under vigorous stirring. Then, 2ml of 30% $TiCl_3$ solution was added and stirred for 30 minutes, resulting in a solution with a $Ti^{4+}$:$Ti^{3+}$ molar ratio of 0.06. The solution was transferred into a Teflon-lined stainless steel autoclave and heated to 180°C for 24 hours under a ramping rate of 10°C $min^{-1}$. The photocatalyst obtained was then washed with ethanol, 0.1M NaOH and DI water, then dried overnight in an oven. Pristine $TiO_2$ was synthesized by calcining the as-synthesized $TiO_{2-x}$ in a furnace at 400°C for 4 hours at 5°C $min^{-1}$ ramping rate.

### 2.3 Characterization

Powder X-ray diffraction (XRD) was conducted using Bruker D8 Discover with Cu Kα radiation (λ=1.54056 Å). Energy dispersive X-ray spectroscopy (EDX) was performed using Hitachi SU8010 under 15kV accelerating voltage.

### 2.4 Photocatalytic Degradation of Polyethylene

Photocatalyst-polyethylene nanocomposite films were prepared using a two-step casting method. In the first step, 150mg of polyethylene powder was added into 20ml of cyclohexane and heated to 70°C under stirring for 1 hour to achieve dissolution. 2ml aliquots were sampled and casted into a 4cm petri dish, then heated to 100°C for 20 minutes to evaporate the solvent, and

dried overnight in an oven at 40°C. In the second step, an appropriate amount of photocatalyst was added into the petri dish to match the amount of polyethylene casted. Then, 3ml of cyclohexane was added and ultrasonicated for 5 minutes at 80°C to disperse the photocatalyst within the polyethylene film. The nanocomposite film was then heated to 100°C for 20 mins to drive off the solvent, and dried overnight in an oven at 40°C.

Photocatalytic polyethylene degradation was performed using a 100W UV395nm LED lamp at an irradiation intensity of 10mW/cm$^2$ for the duration of 2 weeks. The degradation performance was quantified by the mass loss of polyethylene according to Eq. 3

$$Degradation\ (\%) = \frac{m_{PE,\ 0} - m_{PE}}{m_{PE,\ 0}} \times 100\% \quad (3)$$

### 3. DFT results

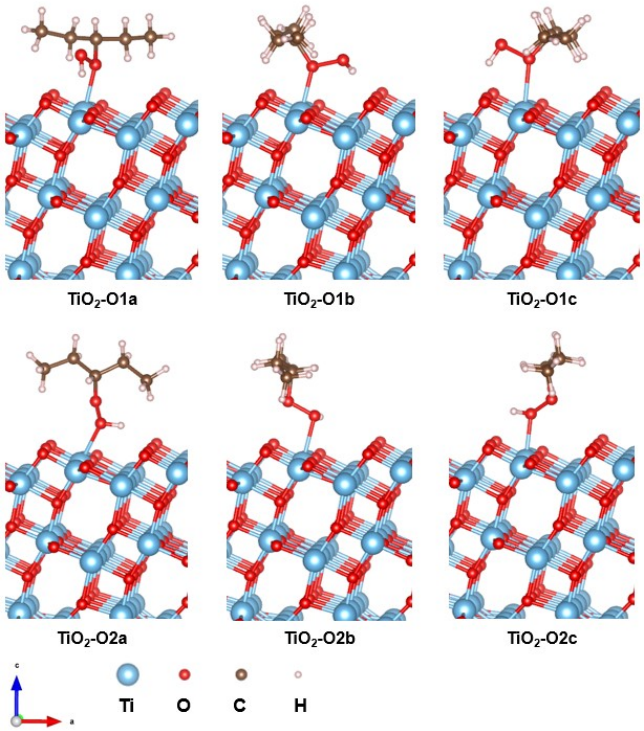


**Figure S1.** Configurations of sec-pentyl hydroperoxide adsorption onto $TiO_2$ surface.

**Table S1.** Comparison of adsorption energies of sec-pentyl hydroperoxide adsorption onto $TiO_2$. Adsorption energies reported are relative to the most stable adsorption configuration $TiO_2$-O2a.

| Adsorption Orientation | Adsorption Energy, $E_{ads}$ (eV) |
|---|---|
| $TiO_2$-O1a | 0.2811 |
| $TiO_2$-O1b | 0.1225 |
| $TiO_2$-O1c | 0.2425 |
| **$TiO_2$-O2a** | **0.0000** |
| $TiO_2$-O2b | 0.4479 |
| $TiO_2$-O2c | 0.2213 |

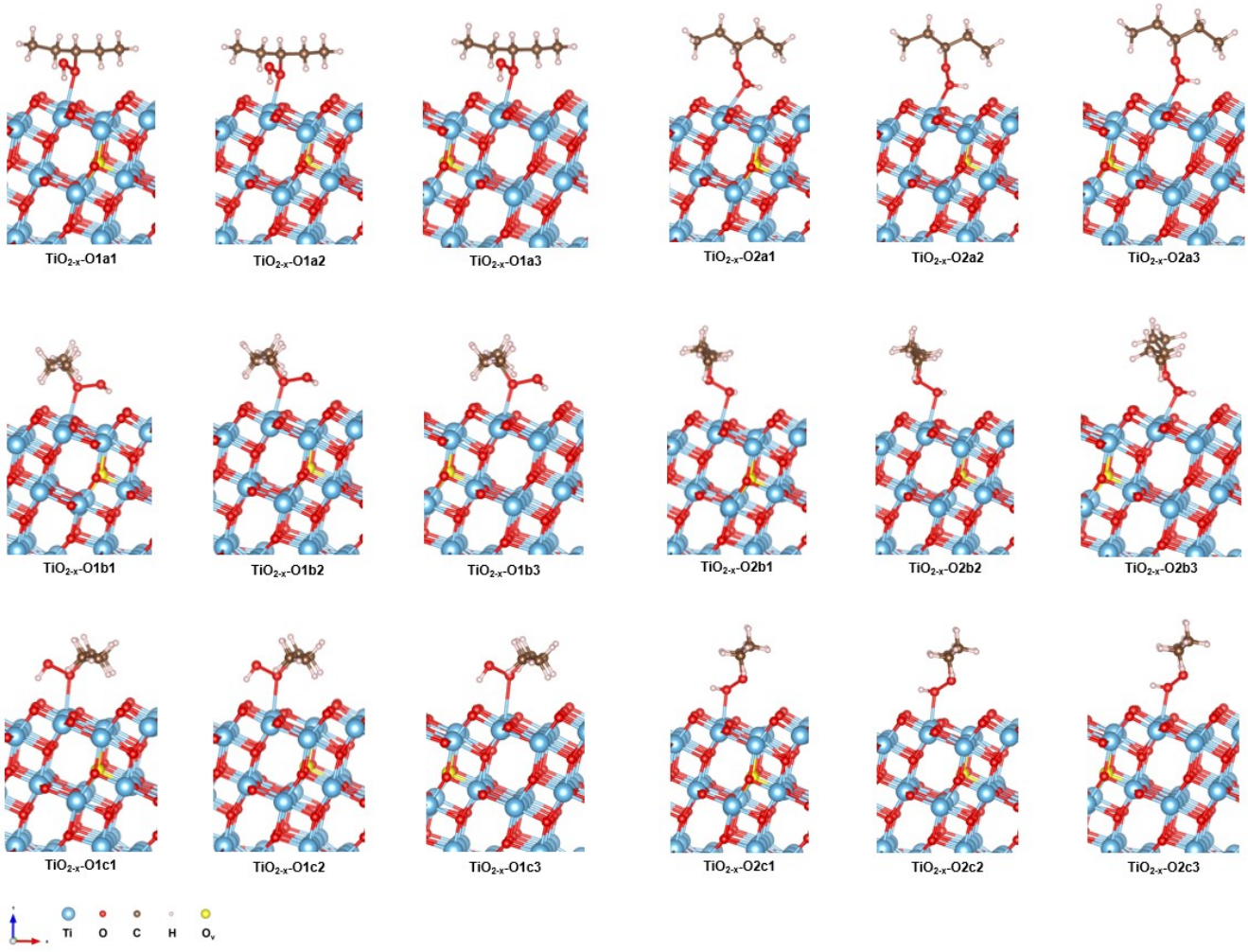


**Figure S2.** Configurations of sec-pentyl hydroperoxide adsorption onto $TiO_{2-x}$ surface.

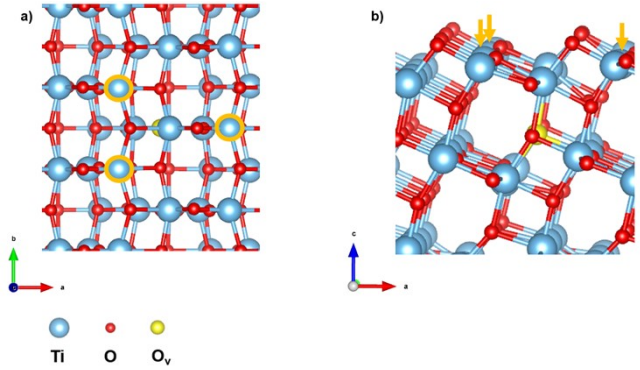


**Figure S3.** a) top view and b) side view of unique adsorption active sites on $TiO_{2-x}$ surface. Orange circle and arrows depict the non-symmetrically equivalent undercoordinated adsorption sites.

**Table S2.** Comparison of adsorption energies of sec-pentyl hydroperoxide adsorption onto $TiO_{2-x}$. Adsorption energies reported are relative to the most stable adsorption configuration $TiO_{2-x}$-O2a1.

| Adsorption Orientation | Adsorption Energy, $E_{ads}$ (eV) |
|---|---|
| $TiO_{2-x}$-O1a1 | 0.2776 |
| $TiO_{2-x}$-O1a2 | 0.3319 |
| $TiO_{2-x}$-O1a3 | 0.5321 |
| $TiO_{2-x}$-O1b1 | 0.1097 |
| $TiO_{2-x}$-O1b2 | 0.2310 |
| $TiO_{2-x}$-O1b3 | 0.3476 |
| $TiO_{2-x}$-O1c1 | 0.2903 |
| $TiO_{2-x}$-O1c2 | 0.2645 |
| $TiO_{2-x}$-O1c3 | 0.4355 |
| **$TiO_{2-x}$-O2a1** | **0.0000** |
| $TiO_{2-x}$-O2a2 | 0.0623 |
| $TiO_{2-x}$-O2a3 | 0.1345 |
| $TiO_{2-x}$-O2b1 | 0.3603 |
| $TiO_{2-x}$-O2b2 | 0.3656 |
| $TiO_{2-x}$-O2b3 | 0.1625 |
| $TiO_{2-x}$-O2c1 | 0.2323 |
| $TiO_{2-x}$-O2c2 | 0.2656 |
| $TiO_{2-x}$-O2c3 | 0.3805 |

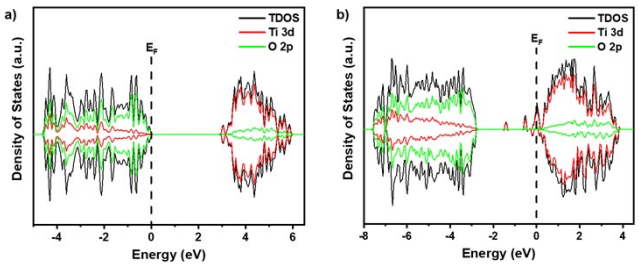


**Figure S4.** Density of states of a) $TiO_2$ and b) $TiO_{2-x}$.

REFERENCES

(1) Kresse, G.; Furthmüller, J. Efficient iterative schemes for ab initio total-energy calculations using a plane-wave basis set. *Physical review B* **1996**, *54* (16), 11169.

(2) Kresse, G.; Hafner, J. Ab initio molecular-dynamics simulation of the liquid-metal–amorphous-semiconductor transition in germanium. *Physical Review B* **1994**, *49* (20), 14251.

(3) Chen, W.; Kuang, Q.; Wang, Q.; Xie, Z. Engineering a high energy surface of anatase $TiO_2$ crystals towards enhanced performance for energy conversion and environmental applications. *RSC Adv.* **2015**, *5* (26), 20396-20409, 10.1039/C5RA00344J. DOI: 10.1039/C5RA00344J.

(4) Cheng, H.; Selloni, A. Surface and subsurface oxygen vacancies in anatase $TiO_2$ and differences with rutile. *Phys. Rev. B* **2009**, *79* (9), 092101. DOI: 10.1103/PhysRevB.79.092101.

(5) Perdew, J. P.; Burke, K.; Ernzerhof, M. Generalized gradient approximation made simple. *Physical review letters* **1996**, *77* (18), 3865.

(6) Blöchl, P. E. Projector augmented-wave method. *Phys. Rev. B* **1994**, *50* (24), 17953-17979. DOI: 10.1103/PhysRevB.50.17953.

(7) Kresse, G.; Joubert, D. From ultrasoft pseudopotentials to the projector augmented-wave method. *Phys. Rev. B* **1999**, *59* (3), 1758-1775. DOI: 10.1103/PhysRevB.59.1758.

(8) Monkhorst, H. J.; Pack, J. D. Special points for Brillouin-zone integrations. *Phys. Rev. B* **1976**, *13* (12), 5188-5192. DOI: 10.1103/PhysRevB.13.5188.

(9) Bader, R. F. Atoms in molecules. *Acc. Chem. Res.* **1985**, *18* (1), 9-15.

(10) Henkelman, G.; Arnaldsson, A.; Jónsson, H. A fast and robust algorithm for Bader decomposition of charge density. *Comput. Mater. Sci.* **2006**, *36* (3), 354-360. DOI: 10.1016/j.commatsci.2005.04.010.

(11) Henkelman, G.; Uberuaga, B. P.; Jónsson, H. A climbing image nudged elastic band method for finding saddle points and minimum energy paths. *J. Chem. Phys* **2000**, *113* (22), 9901-9904. DOI: 10.1063/1.1329672.

(12) Elahifard, M.; Sadrian, M. R.; Mirzanejad, A.; Behjatmanesh-Ardakani, R.; Ahmadvand, S. Dispersion of defects in $TiO_2$ semiconductor: Oxygen vacancies in the bulk and surface of rutile and anatase. *Catalysts* **2020**, *10* (4), 397.

(13) Dudarev, S. L.; Botton, G. A.; Savrasov, S. Y.; Humphreys, C. J.; Sutton, A. P. Electron-energy-loss spectra and the structural stability of nickel oxide: An LSDA+U study. *Phys. Rev. B* **1998**, *57* (3), 1505-1509. DOI: 10.1103/PhysRevB.57.1505.

(14) Linh, N. H.; Nguyen, T. Q.; Diño, W. A.; Kasai, H. Effect of oxygen vacancy on the adsorption of $O_2$ on anatase $TiO_2$(001): A DFT-based study. *Surf. Sci.* **2015**, *633*, 38-45. DOI: 10.1016/j.susc.2014.11.015.

(15) Hammer, B.; Nørskov, J. K. Electronic factors determining the reactivity of metal surfaces. *Surf. Sci.* **1995**, *343* (3), 211-220. DOI: 10.1016/0039-6028(96)80007-0.